J IRAN CHEM SOC (2012) 9:111–119
DOI 10.1007/s13738-011-0044-5

ORIGINAL PAPER

Accelerating the electron transfer of choline oxidase using ionic-liquid/NH_2-MWCNTs nano-composite

Sharareh Sajjadi · Hedayatollah Ghourchian · Hossain-Ali Rafiee-Pour · Parvaneh Rahimi

Received: 26 September 2010 / Accepted: 31 December 2010 / Published online: 19 January 2012

Abstract A nano-composite consisting of amine functionalized multi-walled carbon nanotubes and a room temperature ionic liquid (1-butyl-3-methylimidazolium tetrafluoroborate) was prepared and used for modification of glassy carbon electrode. By immobilizing choline oxidase (ChOx) on the modified electrode, the enzyme direct electron transfer has been achieved. The modified electrode exhibited a pair of well-defined cyclic voltammetric peaks at a formal potential of −0.395 V versus Ag/AgCl in 0.2 M phosphate buffer solution at pH 7.0. This peak was characteristic of ChOx-FAD/$FADH_2$ redox couple. The electrochemical parameters such as charge transfer coefficient (α) and apparent heterogeneous electron transfer rate constant (k_s) were estimated to be 0.36 and 2.74 s^{-1}, respectively. When the enzyme electrode was examined for the detection of choline, a relatively high sensitivity (2.59 μA mM^{-1}) was obtained. Under the optimized experimental conditions, choline was detected in the concentration range from 6.9×10^{-3} to 6.7×10^{-1} mM with a detection limit of 2.7 μM. The peak currents of ChOx were reasonably stable and retained 90% of its initial current after a period of 2 months.

Keywords Choline oxidase · Direct electron transfer · Amine functionalized multi-walled carbon nanotubes · Room temperature ionic-liquid · Choline

S. Sajjadi · H. Ghourchian (✉) · H.-A. Rafiee-Pour
Laboratory of Microanalysis, Institute of Biochemistry and Biophysics, University of Tehran, Tehran, Iran
e-mail: Hadi@ibb.ut.ac.ir

P. Rahimi
Faculty of Chemistry, Center of Excellence in Electrochemistry, University of Tehran, Tehran, Iran

Introduction

Direct electron transfer between redox proteins and electrode surfaces has gained considerable attention in recent years due to its importance in both theoretical [1] and practical [2] applications. Studies based on direct electron transfer of redox enzymes lead to a better understanding of the kinetics and thermodynamics of the biological redox process [1]. Biosensors based on direct electrochemistry of enzymes, so called third generation [3], have some advantages over other types. They usually offer better selectivity by operating in a potential range close to the redox potential of the enzyme itself, thus being less exposed to interfering reactions [4]. These biosensors are also advantageous for in vivo detection due to its simplicity and harmlessness [5].

Choline oxidase (ChOx) as a redox protein is frequently used as biosensing element for quantitative determination of choline. Choline is often considered as a biomarker of cholinergic activity in the brain tissue, especially in early clinical diagnosis of Alzheimer's and Parkinson's diseases [6]. Unfortunately, the third generation biosensor for ChOx has been rarely reported. This may be due to the fact that the redox centers of immobilized ChOx (flavine adenine dinucleotide, FAD) are usually inaccessible to the electrode, because they are deeply buried within the protein [7]. Besides, direct adsorption of enzyme on the electrode surface brings about its denaturation or loss of bioactivity [8]. Therefore, it is necessary to find a host matrix with good biocompatibility which enhances the direct electron transfer between the protein and the underlying electrode, and also provides a favorable microenvironment to keep the bioactivity of the protein. Despite using various matrixes to immobilize ChOx on the electrode [9–13], there are no satisfactory results for its direct electron

transfer. To our knowledge, direct electrochemistry of ChOx was reported only once using didodecyldimethylammonium bromide (DDAB) surfactant film [14] on pyrolytic graphite electrode. But, due to relatively poor electron transfer, further investigation to develop a superior method for promotion of choline oxidase direct electron transfer is still required.

Recently, carbon nanotubes (CNTs) have become an attractive host matrix due to their good biocompatibility, high electrical conductivity, high surface area and significant stability [15–17]. Especially, they can act as electrical connectors between the redox centers of proteins/enzymes and the electrodes and so facilitate direct electron transfer between redox sites of proteins/enzymes and electrode surfaces [18–23].

On the other hand, room temperature ionic liquids (RTILs) belong to a special group of electrolytes consisting entirely of ions that preserve their liquid state around room temperature [24]. They have unique chemical and physical properties such as good stability, no measurable vapor pressure, low toxicity, wide potential window, high ionic conductivity and good solubility [25]. These electrolytes are also compatible with bio-macromolecules and even whole cells [24].

By combination of CNTs and RTILs, a nano-composite is obtained by which all the above mentioned advantages are achieved. The use of CNTs and RTILs at the sensor surface may increase the surface ionic and electrical conductivities and thus enhance the sensitivity of the sensor [26]. The electrodes modified with such a nano-composite were applicable to promote the direct electron transfer of various proteins/enzymes such as glucose oxidase [27], Cytochrome c [28], hemoglobin [29], horseradish peroxidase [30] and catalase [31].

In the present report, an amine functionalized multi-walled carbon nanotube (NH_2-MWCNTs) and a typical RTIL were used as electrode modifier. Then, the modified glassy carbon (GC) electrode was examined for realizing the direct electron transfer of ChOx.

Experimental

Reagents

ChOx (E.C.1.1.3.17) from Alcaligenes species (11 Umg^{-1}), choline chloride and 1-butyl-3-methylimidazolium tetrafluoroborate ([BMIM]BF_4), as a typical RTIL, were purchased from Sigma (St. Louis, MO, USA). MWCNTs, prepared by chemical vapor deposition, were purchased from Chengdu Organic Chemicals Co. Ltd. (Chengdu, China). Potassium phosphate (K_2HPO_4 and KH_2PO_4), ethylenediamine ($C_2H_4[NH_2]_2$) and N,N-dimethylformamide (DMF) were obtained from Merck (Darmstate, Germany). Thionyl chloride ($SOCl_2$) was purchased from Acros Organics. Unless otherwise stated, all samples were prepared in 0.2 M phosphate buffer, pH 7.0 and called as phosphate buffer solution (PBS).

Apparatus and measurements

Electrochemical measurements were performed with a potentiostat/galvanostat (Model 263A, EG&G, USA) controlled by a PowerSuite software package and a GPIB interface. All experiments were performed at room temperature in a conventional electrochemical cell. A three electrode system was used, where a saturated silver/silver chloride (Ag/AgCl) (3 M KCl solution) (from Metrohm) served as the reference electrode; A bare or modified GC electrode with a diameter of 2 mm (from Azar Electrode, Uromia, Iran) and a platinum wire electrode were used as the working and auxiliary electrode, respectively. The surface morphologies of the electrodes were observed through field emission scanning electron microscope (FE-SEM), Hitachi model S-4160.

Preparation of ChOx/RTIL/NH_2-MWCNTs/GC

Prior to use, the GC electrode was carefully polished with 0.3 and 0.05 μm alumina slurry sequentially. The electrode was dried in air after being washed in water. MWCNTs were functionalized according to the procedure described in our previous work [31]. 1.0 mg of NH_2-MWCNTs was dispersed with the aid of ultrasonic agitation in 1 ml of DMF to form a well-dispersed suspension as the stock solution. After approximately 20 min of sonication, uniformly dispersed NH_2-MWCNTs were formed. To obtain the MWCNTs modified GC electrode, 2.5 μl of this suspension was spread evenly onto the surface of the GC electrode. After being air-dried, the NH_2-MWCNTs/GC electrode was immersed into the pure solution of [BMIM]BF_4 for 10 h at 4 C to obtain the RTIL/NH_2-MWCNTs/GC modified electrode. This modified electrode was then immersed in a stock solution of 6 mg/ml ChOx (in PBS 0.2 M, pH 7.0) for 10 h at 4 °C to immobilize the enzyme. The modified electrodes were stored at 4 °C in PBS (pH 7.0) in a refrigerator when not in use.

Results and discussion

Characterization of the surface morphology

FE-SEM was used to characterize the surface morphologies of the modified electrodes. Figure 1a shows FE-SEM image of the GC electrode after deposition of NH_2-MWCNTs. As

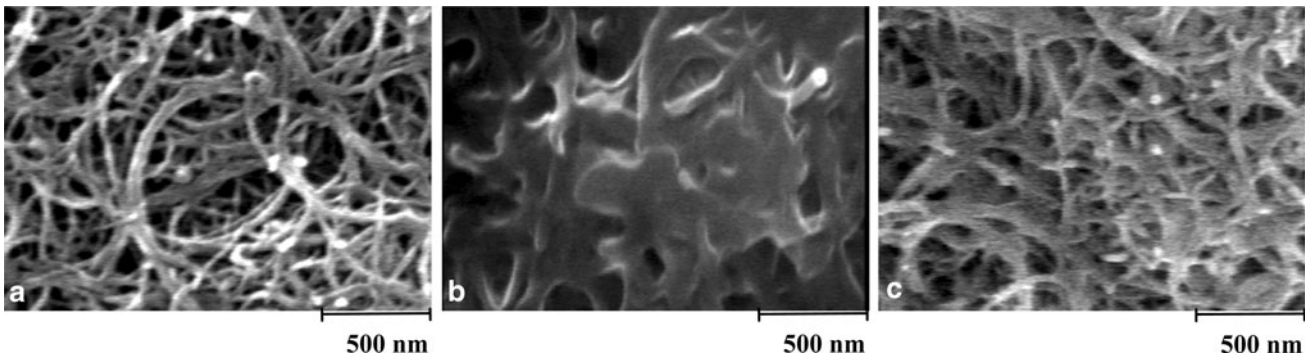

Fig. 1 FE-SEM images of the modified electrodes: **a** NH_2-MWCNTs/GC, **b** RTIL/NH_2-MWCNTs/GC and **c** ChOx/RTIL/NH_2-MWCNTs/GC electrode. The images were taken at the resolution of ×60k

seen, NH_2-MWCNTs were deposited on the electrode surface as bundles, which are tangled with each other (Fig. 1a). Figure 1b shows the image of RTIL/NH_2-MWCNTs modified electrode. A mass of RTIL was embed into the gaps of the formed NH_2-MWCNTs network structure. Comparison between the images a and b indicates that the NH_2-MWNTs are untangled after being treated with RTIL, which is consistent with previous report [32]. From these results, it can be concluded that RTIL plays an important role in the modified electrode. The NH_2-MWNTs were pulled away in RTIL which leads to larger electroactive surface area of the RTIL/NH_2-MWCNTs nano-composite. After immobilization of ChOx/RTIL, the diameter of NH_2-MWCNTs became thicker (Fig. 1c). This could be a sign that ChOx has been successfully immobilized on the surface of RTIL/NH_2-MWCNTs/GC electrode.

Direct electron transfer of ChOx

To consider the electrochemical behavior of ChOx, cyclic voltammetry was used. Figure 2a shows the comparison between the cyclic voltammograms (CVs) of different electrodes in N_2-saturated PBS (0.2 M, pH 7.0). As seen, when ChOx is adsorbed on either bare or RTIL modified GC electrode, it showed no response (Curves a and b, respectively). On the other hand, in the absence of ChOx, the GC electrode modified with either NH_2-MWCNTs or RTIL/NH_2-MWCNTs showed no voltammetric response. These electrodes exhibited only capacitive currents (Curves c and d respectively). When ChOx is immobilized either on NH_2-MWCNTs or RTIL/NH_2-MWCNTs modified electrode, a pair of well-defined redox peak was observed (Curves e and f, respectively). As indicated by the Curves e and f, values of formal potential ($E^{\circ'}$, the average of the cathodic and anodic peak potentials) and peak to peak separation ($\Delta E_p = E_{pa} - E_{pc}$) on both electrodes were almost the same −0.395 V and 60 mV, respectively). These results indicate the role of NH_2-MWCNTs in

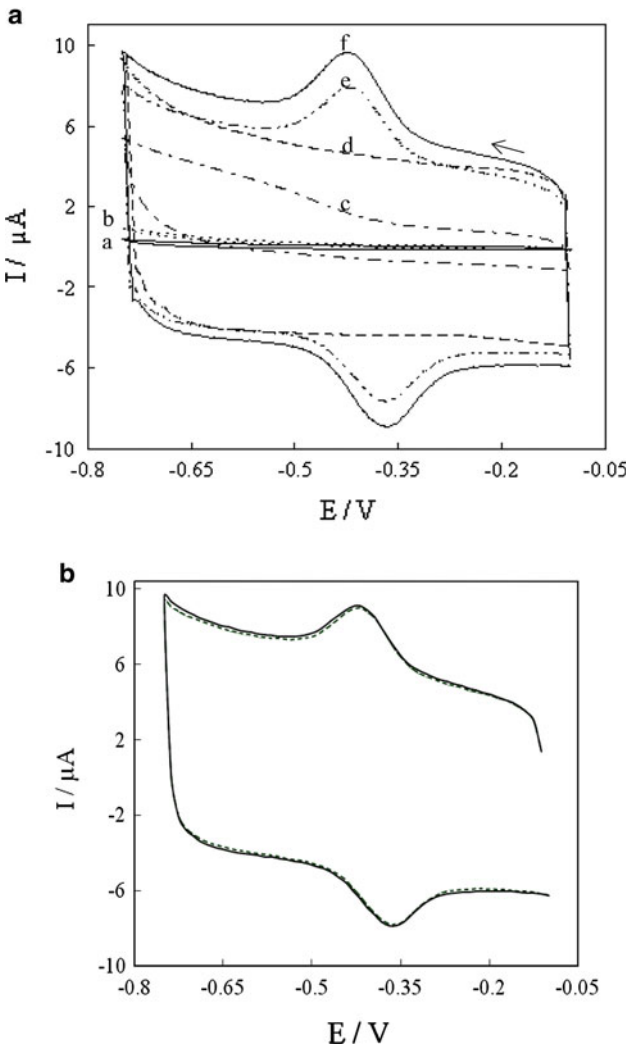

Fig. 2 **a** Cyclic voltammograms of different modified electrodes: *a* ChOx/GC, *b* ChOx-RTIL/GC, *c* NH_2-MWCNT/GC, *d* RTIL/NH_2-MWCNT/GC *e* ChOx/NH_2-MWCN/GC and *f* ChOx/RTIL/NH_2-MWCNT/GC in 0.2 M PBS (pH 7.0) at scan rate of 0.1 Vs^{-1}. **b** Operational stability of the ChOx/NH_2-MWCN/GC electrode: the *solid and dotted lines* show the first and the 100th successive cycle, respectively

mediating the electron transfer between ChOx and the GC electrode. Such a performance could be related to the nanometer dimensions, the electronic structure and the topological defects of CNTs [33]. Meanwhile, CNT increases the effective area of the electrode and consequently the electro-active enzyme loading is greatly improved [34]. Besides, as will be discussed subsequently, the redox transformation of FAD in ChOx is coupled with proton transfer; so the amine groups on MWCNT could provide a vehicle for proton transfer which contributes to increase in conductivity [35]. Increase in the background current after RTIL modifying on the NH_2-MWCNTs may be due to capacitive current of RTIL on NH_2-MWCNTs [27]. ChOx/RTIL/NH_2-MWCNT/GC depicted a pair of well-defined redox peaks at about $E_{pc} = -0.425$ V, $E_{pa} = -0.365$ V, respectively (Curve f). The peak to peak separation of 60 mV and the ratio of anodic to cathodic peak currents almost equal to one suggest that ChOx undergoes a quasi-reversible redox process at the NH_2-MWCNT modified GC electrode. The E° value for ChOx redox reactions on the electrode was calculated to be −0.395 V. This value is consistent with the value reported for ChOx prosthetic group (FAD/$FADH_2$) by Xiao et al. [14].

Stability of ChOx on nano-composite

Long-term stability is one of the most important properties for biosensors. In order to study the long-term storage stability of the modified electrodes, they were stored at 4 °C in 0.2 M PBS (pH 7.0) and the direct electrochemistry of ChOx was tested periodically. ChOx immobilized on NH_2-MWCNTs/GC electrode was not stable enough and lost its electrochemical activity in a couple of days (data not shown) perhaps due to the loss or denaturation of enzyme. However, under the same conditions, the peak currents of ChOx/RTIL/NH_2-MWCNTs/GC electrode were reasonably stable and retained 90% of its initial current after a period of 2 months (data not shown). This shows that RTIL plays an important role in preserving ChOx storage stability. The storage stability of ChOx on RTIL/NH_2-MWCNTs/GC was much better than the previously reported data for ChOx direct electrochemistry [14].

The operational stability of the electrode was also determined by continuous cyclic voltammetry from −0.1 to −0.75 V. The modified electrode preserved 100% of its initial current after 100 cycles (Fig. 2b).

The ability of RTIL to provide a suitable environment for enzymes has been proved elsewhere and correlated to several factors. Polarity of RTIL is one of the most important factors affecting enzyme stability [36]; there is a direct correlation between solvent polarity and enzyme stability [37]. Another factor is the combination of chaotropic (weakly hydrated) cations and kosmotropic (strongly hydrated) anions in hydrophilic RTIL which plays an important role in stabilizing the enzyme in the presence of water [38]. The other factor is hydrogen bond capacity of RTIL which is responsible for maintaining protein's native structure. Enzyme entrapment in the hydrogen bond network of RTIL could prevent its unfolding [36].

The higher stability of ChOx in RTIL may be also ascribed to its possible interactions with NH_2-MWCNT and ChOx. As indicated in some references, the imidazolium ion of RTIL could interact with CNT through π–π, π–cationic, hydrophobic or electrostatic interactions [39, 40]. On the other hand, RTIL can entrap enzyme because multipoint enzyme–RTIL interactions (ionic, hydrogen bonds, van der Waals, etc.) may occur resulting in a supramolecular network able to maintain the protein [41, 42]. Therefore, it seems that the presence of RTIL might play a crucial role in the effective immobilization of ChOx and preserving its native conformation. Therefore, the RTIL/NH_2-MWCNTs nano-composite modified electrode was selected for further studies.

Effect of scan rate

The CVs of ChOx/RTIL/NH_2-MWCNT/GC electrode in N_2-saturated PBS (0.2 M, pH 7.0) at different scan rates (υ) is shown in Fig. 3a. Both of the cathodic (I_{pc}) and anodic (I_{pa}) peak currents increased linearly with increasing the scan rates from 0.01 to 1 Vs^{-1} (Fig. 3b). This suggests a surface-controlled electrode process as expected for immobilized enzyme. The linear regression equations of I_{pc} and I_{pa} versus υ were: I_{pc} (μA) $= 7 \times 10^{-5}$ υ (Vs^{-1}) $+ 3 \times 10^{-6}$, $R^2 = 0.9969$ and I_{pa} (μA) $= 7 \times 10^{-5}$ υ (Vs^{-1}) $+ 2 \times 10^{-6}$, $R^2 = 0.9972$, respectively. The average surface concentration of electroactive ChOx (Γ) adsorbed on the modified electrode was calculated according to the integrated charges (Q) of the cathodic peaks and Faraday's law, $\Gamma = Q/(nFA)$, where n is the number of electrons transferred, F is Faraday's constant and A is the electrode surface area [43]. Using the slope of cathodic peak current versus scan rate, surface concentration of electroactive ChOx was calculated to be 6.6×10^{-10} mol cm^{-2}, suggesting an approximate monolayer of ChOx on the surface of RTIL/NH_2-MWCNT/GC electrode [44].

At scan rates below 200 mVs^{-1}, ΔE_p was found to be approximately 50 mV. This could be a sign for establishment of facile charge transfer kinetics over the range of sweep rates. But at scan rates above 600 mVs^{-1}, ΔE_p increases with increasing the scan rate, indicating the limitation arising from charge transfer kinetics (Fig. 3c).

At small concentration of immobilized species while $\Delta E_p > 200/n$, the kinetic parameters of charge transfer coefficient (α) and apparent charge transfer rate constant (k_s), were calculated using Laviron's Equations [45]:

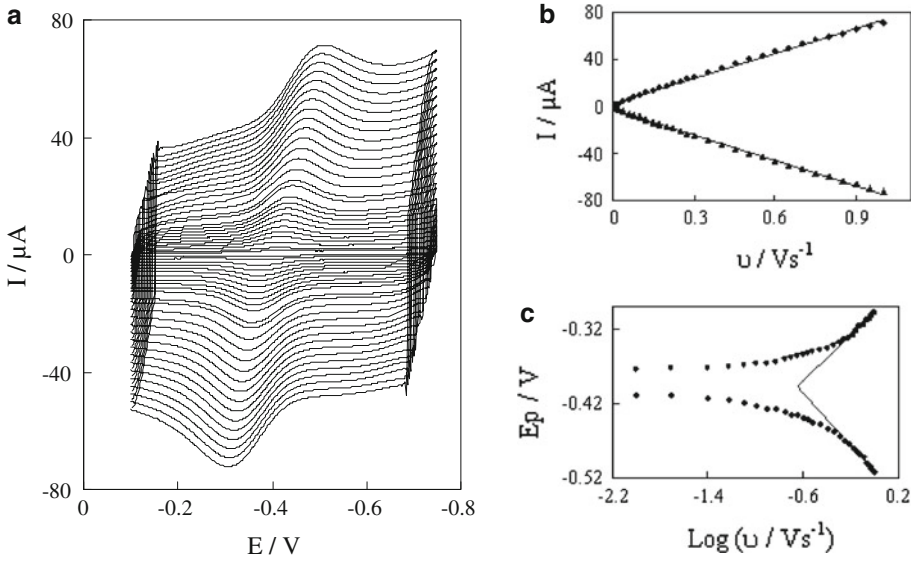

Fig. 3 **a** Cyclic voltammograms of ChOx/RTIL/NH_2-MWCNT/GC electrode at various scan rates. The scan rates (from inner to outer) are 10, 20, 40, 60, 80, 100, 125, 150, 175, 200, 225, 250, 300, 350, 400, 450, 500, 550, 600, 650, 700, 750, 800, 850, 900, 950 and 1,000 mVs^{-1}, respectively. **b** Plot of I_p versus υ. **c** Plot of E_p versus log υ. The experiment was carried out in 0.2 M PBS (pH 7.0)

$$E_{pc} = E^{\circ} + \frac{RT}{\alpha_c nF}\ln\left(\frac{\alpha_c}{m}\right) \quad (1)$$

$$E_{pa} = E^{\circ} + \frac{RT}{\alpha_a nF}\ln\left(\frac{\alpha_a}{m}\right) \quad (2)$$

While, $m = (RT/F)(k_s/v)$

$$\log k_s = \alpha\log(1-\alpha) + (1-\alpha)\log\alpha - \log(RT/nFv) - \alpha(1-\alpha)nF\Delta E_p/2.3RT \quad (3)$$

As indicated by Fig. 3c, at scan rates above 600 mVs^{-1} both E_{pc} and E_{pa} depend linearly on log υ. The graph of $E_p = f$ (log υ) yields two straight lines with slopes of $-2.3RT/\alpha nF$ and $2.3RT/(1-\alpha)nF$ for the cathodic and anodic peaks, respectively [45]. Following these equations, the value of αn was calculated as 0.36 s^{-1}. Given $0.3 < \alpha < 0.7$ in general [46], it could be concluded that $n = 1$ and $\alpha = 0.36$. From the values of ΔE_p (for scan rates above 600 mV s^{-1}) and according to Eq. 3, an average value of k_s for the electron transfer between ChOx and electrode was calculated to be 2.74 s^{-1}.

Influence of the solution pH

The effect of solution pH on the CV of ChOx immobilized on the RTIL/NH_2-MWCNT/GC electrode was studied in the pH range of 5.0–8.7 in N_2-saturated 0.2 M PBS (Fig. 4a). As can be seen in Fig. 4b, the cathodic peak current increased by increasing the pH from 5.0 to 7.0, and then decreased from pH 7.5 to 8.7. The maximum cathodic current obtained in the pH range of 7.0–7.5. So, this range was selected as the optimum pH for studying the direct electron transfer of ChOx. Figure 4c shows that the formal potential ($E^{\circ\prime}$) of the FAD/$FADH_2$ redox couple shifted negatively with increasing the solution pH, indicating that hydrogen ions are involved in the electrode reaction of ChOx. $E^{\circ\prime}$ had a linear relationship with pH with a slope of −59.69 as illustrated in Fig. 4c and could be expressed using Eq. 4:

$$E^{\circ\prime} = -59.689\ \text{pH} + 20.153\ (R^2 = 0.9977) \quad (4)$$

This slope was close to the theoretical value of −59.02 mV pH^{-1} at 25 °C for two protons coupled with two electrons in redox reaction process as expressed in reaction 1.

Biocatalytic activity of ChOx

As known, the direct electron transfer of ChOx is based on the redox transformation of FAD. Figure 5 shows CVs of ChOx immobilized on RTIL/NH_2-MWCNTs/GC electrode in PBS (0.2 M, pH 7.0). In the absence of substrate (oxygen or choline), as indicated by Curve a (Fig. 5), the direct electron transfer of ChOx at the modified electrode could be expressed by Reaction 1.

$$\text{ChOx(FAD)} + 2e^- + 2H+ \rightarrow \text{ChOx}(FADH_2) \quad (1)$$

In the presence of oxygen, the cathodic peak current increased greatly, while the anodic peak current decreased (Fig. 5, Curve b). It seems that both enzyme prosthetic group (FAD) and molecular oxygen contribute in this phenomenon:

On the one hand, oxygen oxidizes ChOx($FADH_2$) based on Reaction 2:

$$\text{ChOx}(FADH_2) + O_2 \rightarrow \text{ChOx(FAD)} + H_2O_2 \quad (2)$$

Through this reaction, the concentration of the reduced form of enzyme (ChOx-$FADH_2$) is decreased while its oxidized form (ChOx-FAD) is increased. Therefore at the electrode surface (Reaction 1), the oxidation peak height is

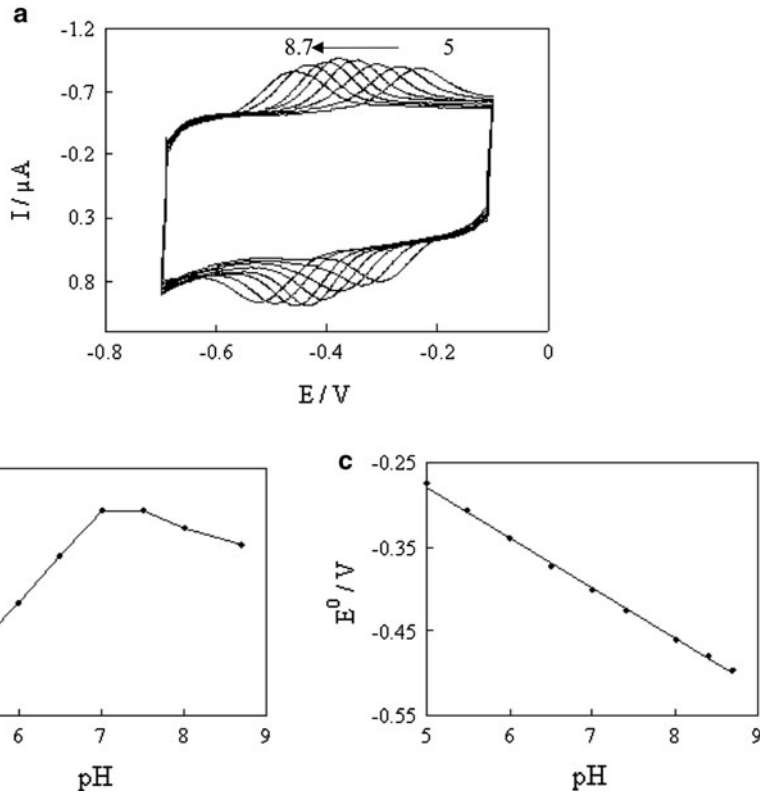

Fig. 4 **a** Cyclic voltammograms of ChOx/RTIL/NH_2-MWCNT/GC electrode at various pH. The pH from right to left is 5, 5.5, 6, 6.5, 7, 7.4, 8, and 8.7, respectively. **b** Plot of I_{pc} versus pH and **c** formal potentials as a function of pH at a scan rate of 0.1 Vs^{-1}. The experiment was carried out in 0.2 M PBS (pH 7.0)

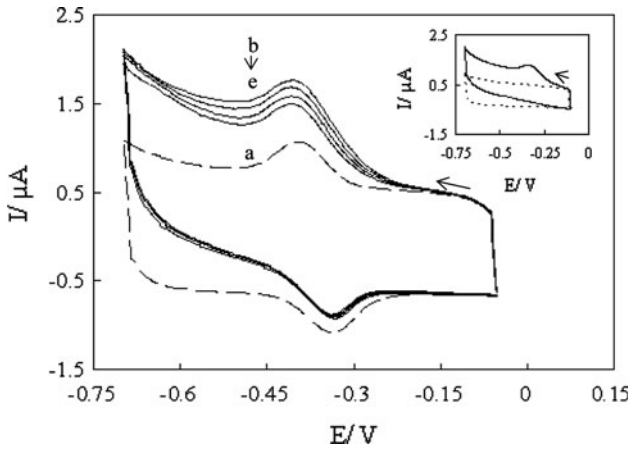

Fig. 5 Cyclic voltammograms of ChOx/RTIL/NH_2-MWCNT/GC electrode in N_2-saturated PBS (*curve a*) and air-saturated PBS containing 0, 0.15, 0.30 and 0.45 mM choline (*curves b–e*, respectively). Inset: *Solid line* shows reduction of oxygen at RTIL/NH_2-MWCNT/GC electrode. *Dotted line* shows CV of the same electrode in the absence of oxygen

reduced while the cathodic peak height is raised (Fig. 5, Curve b).

On the other hand, oxygen molecules are reduced at RTIL/NH_2-MWCNTs/GC electrode in the same potential window (Fig. 5, Inset).

Consequently, both molecular oxygen and enzyme prosthetic group (FAD) contribute to increasing the cathodic peak current (Fig. 5, Curve b).

By addition of choline to the oxygen-saturated PBS, as indicated by Curves c–e (Fig. 5), the cathodic peak current was decreased. This observation could be explained as the following two mechanisms: First, choline oxidation is catalyzed by ChOx according to the Reaction 3:

$$\mathrm{ChOx(FAD)} + \mathrm{choline} \rightarrow \mathrm{ChOx(FADH_2)} + \mathrm{betaine} \quad (3)$$

Theoretically, through the above reaction, the concentration of oxidized form of enzyme (ChOx-FAD) is decreased while its reduced form (ChOx-$FADH_2$) is increased. Therefore according to Reaction 1, the reduction peak height becomes smaller while the oxidation peak height becomes larger (Curve c–e, Fig. 5). Second, the decrease in cathodic current can also be due to the consumption of dissolved oxygen (Reaction 2). All these results indicate the ability of RTIL/NH_2-MWCNTs nanocomposite for retaining the biocatalytic activity of ChOx on GC electrode.

Calibration curve for choline determination

The amperometric responses of the ChOx/RTIL/NH_2-MWCNTs/GC electrode toward successive addition of choline are illustrated in Fig. 6. The response time of the present biosensor was determined to be 6 s as the time required to reach 95% of steady-state current response [47]. As shown in Table 1, this value is significantly smaller than those reported in the literature [12, 13, 48–52]. The

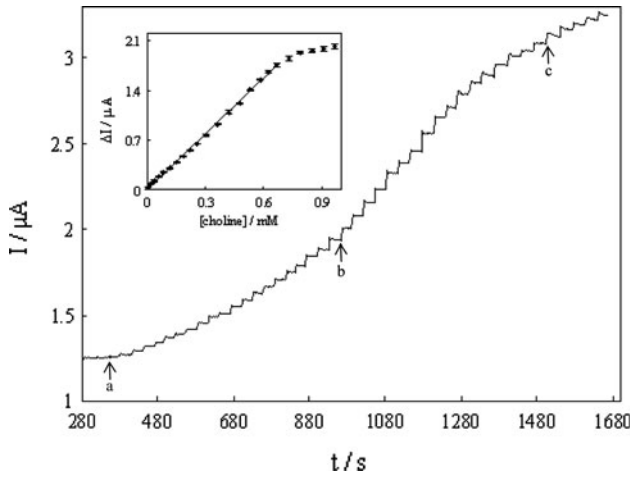

Fig. 6 Amperometric response of ChOx/RTIL/NH2-MWCNT/GC electrode toward successive addition of 1 mM choline in PBS (0.2 M, pH 7.0) at −0.45 V. At each step different volumes of choline were added to electrochemical cell solution (3 mL) as follows: From point *a* to *b*: 5, 10, 15,…, 90, 95 and 100 μl, respectively. From point *b* to *c*: 125, 150, 175,…, 450, 475 and 500 μl, respectively. After point *c*: 950, 1,100, 1,300, 2,000 and 2,200 μl, respectively. The rotation speed was 500 rpm. *Inset* shows the calibration plot for choline detection

faster response may be due to the polarity of RTIL that could increase the solubility of the polar substrate, choline, [42] and effective electron transfer mediation of the nanocomposite. The biosensor response toward choline was linear from 6.9×10^{-3} to 6.7×10^{-1} mM. The linear regression equation was I_{pc} (μA) = 2.5949C (mM) + 0.0058, with a correlation coefficient of 0.998. At higher choline concentrations, a plateau current was observed, showing the characteristics of Michaelis–Menten kinetics. The apparent Michaelis–Menten constant (K_m^{app}) was obtained by using the electrochemical version of the Lineweaver–Burk equation (Eq. 5) [53]:

$$\frac{1}{i_s} = \frac{K_m^{app}}{i_{max}}\left(\frac{1}{C}\right) + \frac{1}{i_{max}} \quad (5)$$

where i_s, i_{max} and C indicate the steady state current after addition of the substrate, maximum current and substrate concentration, respectively. According to the Eq. 5, the K_m^{app} was calculated to be 0.32 mM. The value of K_m^{app} was lower than the values reported for ChOx immobilized by polyvinyl alcohol/Au nano-rod composite (0.78 mM) [51], ChOx cross-linked onto immobilized horseradish peroxidase-carbon paste electrode (0.89 mM) [13], ChOx cross-linked onto over-oxidized polypyrrole and poly(2-naphthol) modified electrode (0.38 mM) [54] and ChOx in DDAB film (0.56 mM) [14]. This comparison indicates that ChOx immobilized on RTIL/NH_2-MWCNTs nanocomposite exhibits a higher biological affinity to choline. The polarity of RTIL could be responsible for increasing the solubility of polar substrate [42] leading to the improvement of the enzyme affinity to choline.

The biosensor sensitivity, obtained from the slope of the calibration curve, was 2.59 μA/mM. This value is higher than those reported for many other choline biosensors [13, 48, 49, 51, 52, 54, 55].

The detection limit (DL) was calculated according to ICH guidelines [http://www.ich.org/fileadmin/Public_Web_Site/ICH_Products/Guidelines/Quality/Q2_R1/Step4/Q2_R1__Guideline.pdf]:

Table 1 Comparison of electroananlytical parameters of the proposed biosensor with other reported choline biosensors

Linear range (M)	DL (M)	Sensitivity (μA/mM)	K_m (mM)	Response time (s)	K_s (s^{-1})	Type of detection	References
1×10^{-6} to 2×10^{-3}	3×10^{-7}	Not reported	Not reported	3	Not reported	Indirect	[10]
1×10^{-5} to 2.1×10^{-3}	Not reported	Not reported	Not reported	Not reported	Not reported	Indirect	[11]
5×10^{-7} to 1×10^{-4}	5×10^{-7}	1.04 to 6.29	0.08	10	Not reported	Indirect	[12]
5×10^{-6} to 6×10^{-4}	3×10^{-6}	0.74	0.89	Less than 15	Not reported	Indirect	[13]
5×10^{-7} to 7×10^{-5}	1×10^{-7}	0.6	Not reported	62, 75 and 80	Not reported	Indirect	[48]
Up to 1.2×10^{-3}	1×10^{-6}	0.48	Not reported	30–50	Not reported	Indirect	[49]
Up to 1.6×10^{-3}	5×10^{-7}	Not reported	Not reported	5	Not reported	Indirect	[56]
Up to 2×10^{-4}	1×10^{-7}	1.60	0.30	Not reported	Not reported	Indirect	[54]
	4×10^{-8}	1.35	0.38				
5×10^{-6} to 1×10^{-4}	7×10^{-7}	Not reported	Not reported	15	Not reported	Indirect	[50]
	1×10^{-7}	9.39	Not reported	8			
Up to 5×10^{-3}	1×10^{-5}	1.99	Not reported	Not reported	Not reported	Indirect	[55]
2×10^{-5} to 4×10^{-4}	1×10^{-5}	0.12	0.78	Less than 20	Not reported	Indirect	[51]
5×10^{-6} to 8×10^{-4}	5×10^{-6}	1.25	0.228	60	Not reported	Indirect	[52]
1×10^{-5} to 1×10^{-4}	5×10^{-6}	Not reported	0.56	Not reported	Not reported	Direct	[14]
6.9×10^{-6} to 6.7×10^{-4}	2.7×10^{-6}	2.59	0.32	6	2.74	Direct	This work

DL = 3.3 σ/S, where σ is the standard deviation of the response and S is the slope of calibration curve. The DL was determined to be 2.7 μM. Although there were some lower values of DL obtained by indirect methods [10, 12, 48–50, 54, 56], the DL obtained in the present work is comparable and in some cases it is better than those of the previously reported indirect choline biosensors [13, 51, 52, 55]. Besides, this value was about two times lower than that reported by Xiao et al. [14] for direct choline detection. The reproducibility of the biosensor response at 0.22 mM choline concentration was examined between five different electrodes and the relative standard deviation was calculated to be 2.4%. A comparison of the analytical parameters for choline detection is summarized in Table 1.

Conclusion

Using the RTIL/NH_2-MWCNTs nano-composite a suitable microenvironment for ChOx direct electron transfer was prepared. It seems that the nano-composite plays a dual role for direct electron transfer between ChOx and GC electrode; Principally, the MWCNTs portion plays as a promoter for electron transfer while RTIL fraction maintains the ChOx native structure. RTIL also plays as a linker between CNT and ChOx which leads to further stabilization of the protein. The polarity of RTIL increases the solubility of choline which leads to a faster reaction. Attractive features such as fast response time, small value of K_m^{app}, reasonable reproducibility, high sensitivity and long-term stability relative to the data reported in the literature, make the third-generation choline biosensor a potential candidate for commercial purposes.

Acknowledgments Financial supports provided by the Research Council of the University of Tehran and Iran National Science Foundation (INSF) are gratefully appreciated.

References

1. C. Leger, P. Bertrand, Chem. Rev. **108**, 2379 (2008)
2. Y. Wu, S. Hu, Microchim. Acta **159**, 1 (2007)
3. X.H. Kang, J. Wang, Z.W. Tang, H. Wu, Y.H. Lin, Talanta **78**, 120 (2009)
4. R.S. Freire, C.A. Pessoa, L.D. Mello, L.T. Kubota, J. Brazil. Chem. Soc. **14**, 230 (2003)
5. J. Wang, Chem. Rev. **108**, 814 (2008)
6. M. Klingner, J. Apelt, A. Kumar, D. Sorger, O. Sabri, J. Steinbach, M. Scheunemann, R. Schliebs, Int. J. Dev. Neurosci. **21**, 357 (2003)
7. O. Quaye, G.T. Lountos, F. Fan, A.M. Orville, G. Gadda, Biochemistry **47**, 243 (2008)
8. X. Lu, Z. Wen, J. Li, Biomaterials **27**, 5740 (2006)
9. L. Campanella, M.P. Sammartino, M. Tomassetti, Anal. Lett. **22**, 1389 (1989)
10. F. Qu, M. Yang, J. Jiang, G. Shen, R. Yu, Anal. Biochem. **344**, 108 (2005)
11. Y.H. Bai, Y. Du, J.J. Xu, H.Y. Chen, Electrochem. Commun. **9**, 2611 (2007)
12. H. Shi, Y. Yang, J. Huang, Z. Zhao, X. Xu, J.I. Anzai, T. Osa, Q. Chen, Talanta **70**, 852 (2006)
13. M. Yang, Y. Yang, Y. Yang, G. Shen, R. Yu, Anal. Biochem. **334**, 127 (2004)
14. H. Xiao, T. Liu, N. Zhou, Z. Yu, G. Li, Sens lett **6**, 209 (2008)
15. J. Wang, M. Musameh, Anal. Chem. **75**, 2075 (2003)
16. J. Wang, Electroanalysis **17**, 7 (2005)
17. M. Valcárcel, S. Cárdenas, B.M. Simonet, Anal. Chem. **79**, 4788 (2007)
18. J.J. Davis, R.J. Coles, H.A.O. Hill, J. Electroanal. Chem. **440**, 279 (1997)
19. Y.D. Zhao, W.D. Zhang, H. Chen, Q.M. Luo, S.F.Y. Li, Sens. Actuators B **87**, 168 (2002)
20. C.X. Cai, J. Chen, Anal. Biochem. **332**, 75 (2004)
21. Y.Y. Sun, F. Yan, W.S. Yang, C.Q. Sun, Biomaterials **27**, 4042 (2006)
22. M. Viticoli, A. Curulli, A. Cusma, S. Kaciulis, S. Nunziante, L. Pandolfi, F. Valentini, G. Padeletti, Mater. Sci. Eng. C **26**, 947 (2006)
23. A. Salimi, E. Sharifi, A. Noorbakhsh, S. Soltanian, Biosens. Bioelectron. **22**, 3146 (2007)
24. D. Wei, A. Ivaska, Anal. Chim. Acta **607**, 126 (2008)
25. M.C. Buzzeo, C. Hardacre, R.G. Compton, Anal. Chem. **76**, 4583 (2004)
26. A.J. Saleh Ahammad, J.J. Lee, M.A. Rahman, sensors 9, 2289 (2009)
27. R. Gao, J. Zheng, Electrochem. Commun. **11**, 608 (2009)
28. C. Xiang, Y. Zou, L.X. Sun, F. Xu, Electrochem. Commun. **10**, 38 (2008)
29. W. Wei, H.H. Jin, G.C. Zhao, Microchim. Acta **164**, 167 (2009)
30. P. Du, S. Liu, P. Wu, C. Cai, Electrochim. Acta **52**, 6534 (2007)
31. P. Rahimi, H.A. Rafiee-Pour, H. Ghourchian, P. Norouzi, M.R. Ganjali, Biosens. Bioelectron. **25**, 1301 (2010)
32. X. Liu, Z. Ding, Y. He, Z. Xue, X. Zhao, X. Lu, Coll. Surf. B **79**, 27 (2010)
33. P.J. Britto, K.S.V. Santhanam, A. Rubio, J.A. Alonso, P.M. Ajayan, Adv. Mater. **11**, 154 (1999)
34. Y. Yan, W. Zheng, M. Zhang, L. Wang, L. Su, L. Mao, Langmuir **21**, 6560 (2005)
35. L. Valentini, I. Armentano, D. Puglia, J.M. Kenny, Carbon **42**, 323 (2004)
36. P.C.A.G. Pinto, M.L.M.F.S. Saraiva, J.L.F.C. Lima, Anal. Sci. **24**, 1231 (2008)
37. O. Ulbert, K. Bélafi-Bakó, K. Tonova, L. Gubicza, Biocatal. Biotransform. **23**, 177 (2005)
38. E. Fehér, B. Major, K. Bélafi-Bakó, L. Gubicza, Biochem. Soc. Trans. **35**, 1624 (2007)
39. Q. Zhao, D. Zhan, H. Ma, M. Zhang, Y. Zhao, P. Jing, Z. Zhu, X. Wan, Y. Shao, Q. Zhuang, Front. Biosci. **10**, 326 (2005)
40. T. Fukushima, T. Aida, Chem. Eur. J. **13**, 5048 (2007)
41. C.F. Poole, J. Chromatrogr. A **1037**, 49 (2004)
42. S. Park, R.J. Kazlauskas, Curr. Opin. Biotech. **14**, 432 (2003)
43. A.J. Bard, L.R. Faulkner, *Electrochemical Methods: Fundamentals and Applications*, 2nd edn. edn. (John Wiley & Sons, New York, 2001)
44. A. Merz, *Electrochemistry IV* (Springer, Berlin, 1990)
45. E. Laviron, J. Electroanal. Chem. **101**, 19 (1979)
46. H. Ma, N. Hu, J.F. Rusling, Langmuir **16**, 4969 (2000)
47. D. Ragupathy, A.l. Gopalan, K.P. Lee, Electrochem. Commun. **11**, 397 (2009)
48. S.S. Razola, S. Pochet, K. Grosfils, J.M. Kauffmann, Biosens. Bioelectron **18**, 185 (2003)

49. S. Şen, A. Gülce, H. Gülce, Biosens. Bioelectron. **19**, 1261 (2004)
50. Z. Song, J.D. Huang, B.Y. Wu, H.B. Shi, J.I. Anzai, Q. Chen, Sens. Actuators B **115**, 626 (2006)
51. X. Ren, F. Tang, R. Liao, L. Zhang, Electrochim. Acta **54**, 7248 (2009)
52. T. Shimomura, T. Itoh, T. Sumiya, F. Mizukami, M. Ono, Talanta **78**, 217 (2009)
53. J. Li, S.N. Tan, H. Ge, Anal. Chim. Acta **335**, 137 (1996)
54. A. Guerrieri, V. Lattanzio, F. Palmisano, P.G. Zambonin, Biosens. Bioelectron. **21**, 1710 (2006)
55. B.C. Hsieh, K. Matsumoto, T.J. Cheng, G. Yuu, R.L.C. Chen, J. Pharmaceut. Biomed. Anal. **45**, 673 (2007)
56. M. Yang, Y. Yang, Y. Yang, G. Shen, R. Yu, Anal. Chim. Acta **530**, 205 (2005)